Free Radical Biology and Medicine 134 (2019) 484–497

Contents lists available at ScienceDirect

Free Radical Biology and Medicine

journal homepage: www.elsevier.com/locate/freeradbiomed

Original article

Poricoic acid A enhances melatonin inhibition of AKI-to-CKD transition by regulating Gas6/Axl−NF−κB/Nrf2 axis

Dan-Qian Chen[a,1], Ya-Long Feng[a,1], Lin Chen[a], Jing-Ru Liu[a], Ming Wang[a], Nosratola D. Vaziri[b], Ying-Yong Zhao[a,*]

[a] School of Pharmacy, Faculty of Life Science & Medicine, Northwest University, No. 229 Taibai North Road, Xi'an, Shaanxi, 710069, China
[b] Division of Nephrology and Hypertension, School of Medicine, University of California Irvine, Irvine, CA, 92897, USA

ARTICLE INFO

Keywords:
Poricoic acid A
Melatonin
Poria cocos
Acute kidney injury
Chronic kidney disease
Gas6/Axl
Inflammation and oxidative stress

ABSTRACT

Renal ischemia-reperfusion injury (IRI) is a complex syndrome, which causes chronic kidney disease (CKD) after recovery from IRI-mediated acute kidney injury (AKI). There is no single therapy that could effectively prevent the renal injury after ischemia. In this study, the effects of melatonin or poricoic acid A (PAA) and their combination were investigated in protecting against AKI-to-CKD transition in rats and hypoxia/reoxygenation (H/R)-induced injury in cultured renal NRK-52E cells. Melatonin and PAA significantly reduced the magnitude of rise in serum creatinine and urea levels in IRI rats at days 3 and 14. Our results further showed that treatment with melatonin and PAA ameliorated renal fibrosis and podocyte injury by attenuating oxidative stress and inflammation *via* regulation of nuclear factor-kappa B (NF-κB) and nuclear factor-erythroid-2-related factor 2 (Nrf2) pathways in IRI rats. Melatonin and PAA protected against AKI-to-CKD transition by regulating growth arrest-specific 6 (Gas6)/Axl−NF−κB/Nrf2 signaling cascade. Melatonin and PAA initiallyupregulated Gas6/Axl signaling to reduce oxidative stress and inflammation in AKI and subsequently downregulated Gas6/Axl signaling to attenuate renal fibrosis and progression to CKD. Melatonin and PAA inhibited expression of extracellular matrix proteins. Poricoic acid A enhances melatonin-mediated inhibition of AKI-to-CKD transition by the regulating Gas6/Axl−NF−κB/Nrf2 signaling cascade. Notably, our study first identified Axl as a promising therapeutic target for prevention of AKI-to-CKD transition.

1. Introduction

Acute kidney injury (AKI) is characterized by the rapid loss of kidney function leading to the accumulation of end products such as creatinine and urea as well as reduced urine output [1]. Even if the patients with AKI survive from the acute stage, the mortality rates of which are reportedly 30%–70%, AKI confers an important risk for development of chronic kidney disease (CKD) and its progression to end-stage renal disease [2]. Renal ischemia-reperfusion injury (IRI) is one of the most common causes of AKI, which subsequently leads to CKD, such as hypertensive nephropathy, obstructive nephropathy, glomerulonephritis and diabetic nephropathy [2]. Renal IRI has been considered as a proper model to explore the effect of therapeutic interventions on AKI-to-CKD transition [3].

The mechanisms underlying renal IRI are associated with the initiation of oxidative stress and inflammation, which are regulated by the growth arrest-specific 6 (Gas6) and its receptors Tyro3, Axl and MerTK, among which Gas6 exerts its anti-inflammatory effects mainly through Axl [4]. In acute stage, Gas6/Axl plays protective roles after IRI in multiple organs, including kidney, heart and liver [5]. Gas6/Axl regulates oxidative stress and inflammation through its downstream mediators, including nuclear factor-kappa B (NF-κB). NF-κB and nuclear factor-erythroid-2-related factor 2 (Nrf2) are the two key transcription factors that regulate cellular responses to oxidative stress and inflammation [6]. Oxidative stress and inflammation are inseparably linked as they generate a vicious cycle in which oxidative stress triggers inflammation, which results in the activation and recruitment of immune cells. Inflammation, in turn, triggers oxidative stress through production of reactive oxygen species, reactive nitrogen species and halogen species by the activation of leukocytes and resident cells. These vicious events accelerate tissue injury by promoting apoptosis, necrosis and fibrosis [7]. However, in CKD, Gas6/Axl serves as a pro-fibrotic route and accelerates fibrogenesis [8]. The role of Gas6/Axl during AKI-to-CKD transition in renal IRI needs to be clarified.

* Corresponding author. School of Pharmacy, Faculty of Life Science & Medicine, Northwest University, No. 229 Taibai North Road, Xi'an, Shaanxi, 710069, China.
E-mail addresses: zyy@nwu.edu.cn, zhaoyybr@163.com (Y.-Y. Zhao).
[1] These authors contributed equally to this work.

https://doi.org/10.1016/j.freeradbiomed.2019.01.046
Received 1 October 2018; Received in revised form 31 January 2019; Accepted 31 January 2019
Available online 02 February 2019

Abbreviations

12-LO	12-lipoxygenase
5-HTP	5-hydroxytryptophan
5-MTP	5-methoxytryptophan
AKI	acute kidney injury
COX-2	cyclooxygenase-2
CTL	control
DAPI	40, 6-diamino-2-phenylindole
ECM	extracellular matrix
EMT	epithelial-mesenchymal transition
FSP1	fibroblast-specific protein 1
Gas6	growth arrest-specific 6
GCLC	glutamate cysteine ligase catalytic subunit
H&E	hematoxylin & eosin
H/R	hypoxia/reoxygenation
HO-1	heme oxygenase-1
iNOS	inducible nitric oxide synthase
IRI	ischemia-reperfusion injury
IκBα	inhibitor of kappa B alpha
MCP-1	monocyte chemoattractant protein-1
NF-κB	nuclear factor-kappa B
NQO-1	NAD(P)H quinoneoxidoreductase 1
Nrf2	nuclear factor-erythroid-2-related factor 2
PAA	poricoic acid A
p-IκBα	phosphorylated-IκBα
qRT-PCR	quantitative real-time polymerase chain reaction
Rac1	Ras-related C3 botulinum toxin substrate 1
SLPC	surface layer of *Poria cocos*
TGF-β1	transforming growth factor beta 1
α-SMA	alpha smooth muscle actin

Melatonin from pineal gland serves as a synchronizer of the biological clock and plays beneficial roles in ameliorating oxidative stress and inflammation in multiple organs, such as heart, brain, liver and lung. A clinical investigation reported that the amplitude and rhythm of melatonin decreases in advanced CKD [9]. Melatonin is also involved in the protection against renal IRI under various pathological conditions [10]. Recently, the combined use of melatonin and other drugs or natural products has been investigated in several diseases [11,12]. However, studies on the effect of combined medication against renal IRI are far from sufficient.

Natural products as a therapy source have been widely applied to anti-fibrosis including renal fibrosis [13–15]. *Poria cocos* Wolf (Polyporaceae) is a well-known traditional medicinal fungus that grows around the roots of pine trees in Asia and North America [16]. The inner parts of *P. cocos* are commonly used to treat edema, nephrosis, dizziness, nausea and emesis [16]. The chemical constituents obtained from *P. cocos* are mainly triterpenoids [16]. However, the triterpenoid compounds are the main components of the surface layer of *P. cocos* (SLPC) that exhibited a strong diuretic effect [17,18]. Our previous studies revealed that treatment with SLPC ameliorated CKD by improving abnormal amino acid and lipid metabolisms [19,20]. However, it remains to be clarified whether SLPC and its components can exert beneficial roles in renal IRI. Poricoic acid A (PAA) is a major component of SLPC. The present study was undertaken to test the hypothesis that the combination of melatonin and PAA may show better renoprotective effects on AKI-to-CKD transition than each agent alone *via* the regulation of Gas6/Axl—NF—κB/Nrf2 signaling cascade. Based on this hypothesis, this study was designed to investigate the effects of the combination of melatonin and PAA on AKI-to-CKD transition and explore their underlying mechanisms.

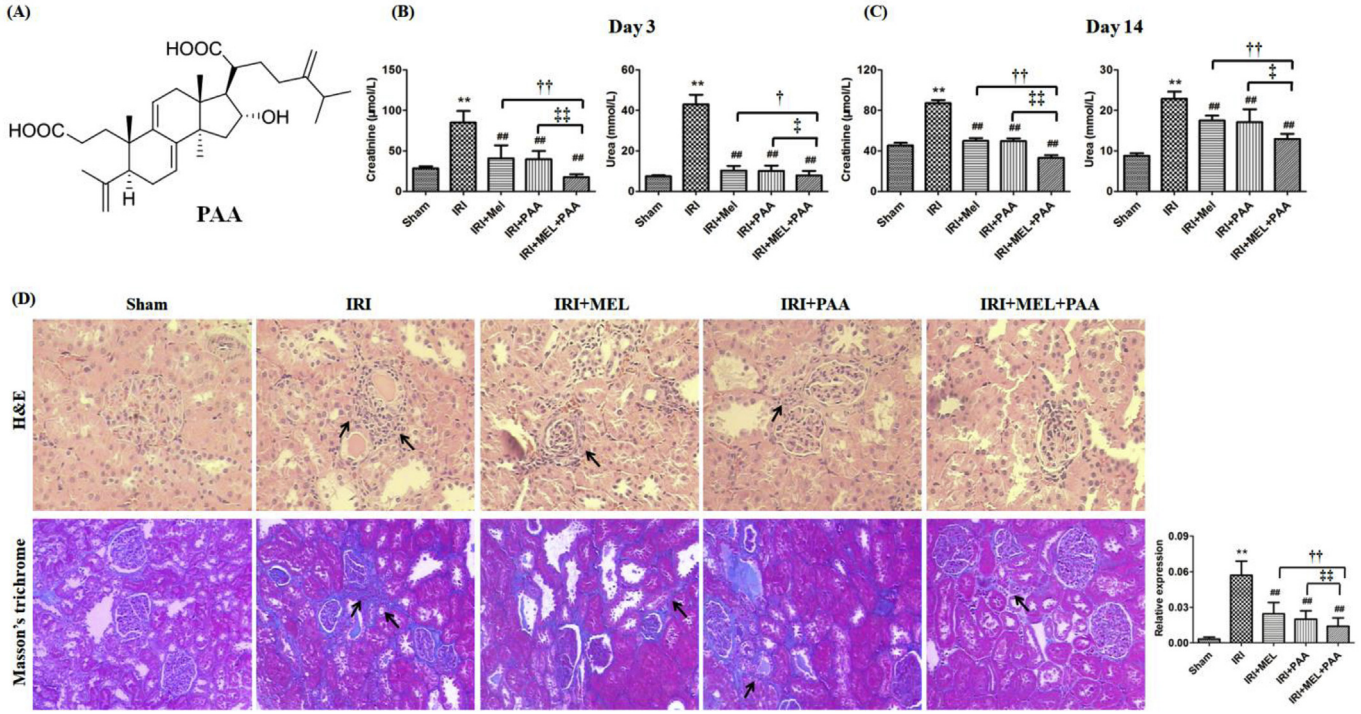

Fig. 1. The renoprotective effects of melatonin and PAA on IRI rats. (A) The chemical structure of PAA. (B) Serum creatinine and urea levels in different groups at day 3 after IRI procedure. (C) Serum creatinine and urea levels in different groups at day 14 after IRI procedure. (D) Representative micrographs of HE and masson's trichrome staining in indicated groups at day 14 after IRI procedure. Each data represented as the mean ± SD (n = 7). Magnification, ×400, HE; ×100, Masson's trichrome. $^{**}P < 0.01$ versus sham group. $^{\#\#}p < 0.01$ versus IRI group. $^{\dagger}p < 0.05$; $^{\dagger\dagger}p < 0.01$ versus IRI + melatonin group. $^{\ddagger}p < 0.05$; $^{\ddagger\ddagger}p < 0.01$ versus IRI + PAA group.

2. Methods

2.1. Materials and methods

Melatonin was purchased from Sigma-Aldrich (M5250, St. Louis, MO, USA). SLPC was purchased from Shaanxi Medicinal Materials Company (Xi'an, Shaanxi, China). The cell counting kit-8 (E1CK-000208) was purchased from EnoGene (Shanghai, China). 40, 6-Diamino-2-phenylindole (DAPI) was purchased from Roche (Mannheim, Badenia-wirtembergia, Germany). DMEM/F-12, fetal bovine serum and Lipofectamine RNAiMAX were purchased from Thermo Fisher Scientific (New York, New York, USA).

2.2. Extraction and isolation of PAA

SLPC (20 kg) was powdered and extracted with 95% ethanol (100 L) three times. The solvent was removed under reduced pressure and crude extracts were obtained. The crude extracts (830 g) was subsequently dissolved in water and successively partitioned with petroleum ether, ethyl acetate, and n-butanol to yield three fractions. The ethyl acetate fraction (500 g) was performed on MCI gel CHP20P eluted with a gradient system of methanol-H_2O (from 50:50 to 100:0) and yielded five fractions A-F. Fraction C (60 g) was subjected to normal-phase fractionation on silica gel column chromatography using dichloromethane-methanol (from 100:1 to 1:1) and yielded seven fractions C1-C7. Fraction C4 (12.1 g) was purified over RP-18 column chromatography using methanol-H_2O elution system (from 50:50 to 100:0) and yielded fractions C41-C43. C42 (6.0 g) was then purified by reverse-phase semi-preparative high-performance liquid chromatography applying a methanol-H_2O (85:15) elution system and a flow rate of 3 mL/min for 25 min. PAA (1.6 g) was obtained and its chemical structure was shown in Fig. 1A.

2.3. Animals and treatment

All animal care and experimental procedures was carried out in strict accordance with the recommendations in the Guide for the Care and Use of Laboratory Animals of the State Committee of Science and Technology of the People's Republic of China. The protocol was approved by the Committee on the Ethics of Animal Experiments of the Northwest University (Permit Number: SYXK 2010-004). Male Sprague-Dawley rats (180–200 g) rats were purchased from the Central Animal Breeding House of Fourth Military Medical University (Xi'an, Shaanxi, China). Rats were equally and randomly divided into five groups: sham, IRI, IRI + melatonin, IRI + PAA, and IRI + melatonin + PAA group. Before surgery, rats were anesthetized by 10% chloral hydrate. IRI model were performed by clamping the renal pedicles for 1 h using nontraumatic bulldog clamp, while sham-operated rats received laparotomy only. Melatonin was given to IRI rat as previous described with little modification [21]. Melatonin (20 mg/kg) was given by intraperitoneal injection at 30 min after reperfusion and then melatonin (50 mg/kg) was also administered at 6-h and 18-h after reperfusion. Additionally, melatonin (50 mg/kg) was repeatedly administrated from day 2 to day 7 after reperfusion. The PAA (10 mg/kg per day) by oral administration showed better renal protective effect based on our previous experiments (data not shown). The PAA (10 mg/kg) was administrated by intragastric administration from 2 to day 13 after reperfusion.

2.4. Serum biochemical analysis

After sacrificed, serum creatinine and urea were tested by the AU6402 automatic analyzer (Olympus Corporation, Tokyo, Japan).

2.5. Cell culture and treatment

Normal rat kidney proximal tubular epithelial cells (NRK-52E), purchased from the China Center for Type Culture Collection, were employed to investigate the beneficial effect of melatonin and PAA in hypoxia/reoxygenation (H/R)-induced injury. NRK-52E cells were cultured in DMEM/F-12 with 10% fetal bovine serum at 37 °C with 5% CO_2. The cells were divided into seven groups: Control (CTL), H/R, melatonin, PAA, H/R + melatonin, H/R + PAA, H/R + melatonin + PAA. H/R cells were placed in the hypoxic hamber under 1% O_2 atmosphere at 37 °C for 9 h, and then placed in normal situation for 6 or 12 h for reoxygenation. During reoxygenation, the treated groups were incubated with melatonin (10 μM) and PAA (10 μM). After experiment, NRK-52E cells were harvested for cell viability analysis, quantitative real-time polymerase chain reaction (qRT-PCR), western blot and immunofluorescence staining.

2.6. Analysis of cell viability by cell counting kit-8

The 1×10^4 cells cultured in 96-well plates were treated with different concentrations of PAA (0, 1, 10, 50, 100 μM) for 24 h. The cell counting kit-8 kit was employed to measure cell viability according to the manufacturer's protocol. The absorbance at 450 nm was detected by a microplate reader (Thermo Fisher Scientific, New York, New York, USA). The results of cell viability for each concentration were repeated six times.

2.7. Knockdown of Axl by siRNA

Axl siRNA and negative control siRNA were designed and synthesized by Sangon (Shanghai, China), and transfected into NRK-52E cells grown in 6-well plates by Lipofectamine RNAiMAX according to the manufacturer's guide. After 72 h incubation, the cells were collected for the next experiments.

2.8. Immunohistochemical staining

Paraffin-embedded rat kidney sections (5-μm thickness) were prepared as a routine procedure. The sections were stained with Hematoxylin & eosin (H&E), Masson's trichrome staining and picrosirius red reagent by standard protocol [22]. The sections were deparaffinized by three xylene washes and hydrated by alcohol and washed in distilled water. Three percent hydrogen peroxide was employed to block endogenous peroxidase activity. Antigen retrieval was performed by a microwave oven for 15 min in a citrate buffer (10 mM, pH 6.0). After washing in distilled water and phosphate buffer saline, sections were incubated with 5% BSA at room temperature for 30 min. Then, sections were incubated with primary antibodies against ED-1 (1:100, ab125212, Abcam, Cambridge, MA,USA), CD3 (1:100, ab5690, Abcam, Cambridge, MA,USA), NF-κB p65 (1:150, ab16502, Abcam, Cambridge, MA,USA), inducible nitric oxide synthase (iNOS, 1:100, ab15323, Abcam, Cambridge, MA, USA) and TGF-β1 (1:100, ab92486, Abcam, Cambridge, MA,USA) at 4 °C overnight. Negative controls included omitting the primary antibody. After being washed with phosphate buffer saline, the sections were incubated with a secondary antibody at room temperature for 2 h. The reaction was visualized with diaminobenzidine. Counterstaining was performed with 50% Harris hematoxylin. The sections were mounted with neutral gum. Image analysis was done by using Image-Pro Plus 6.0 software.

2.9. Immunofluorescence staining and confocal microscopy

Kidney cryosections (8-μm thickness) or NRK-52E cells cultured on coverslips were fixed with 4% paraformaldehyde for 10 min at room temperature. The slides were blocked with 10% goat serum for 30 min, then immunostained with primary antibodies against alpha smooth

muscle actin (α-SMA, 1:100, ab7817, Abcam, Cambridge, MA, USA), E-cadherin (1:500, ab76055, Abcam, Cambridge, MA, USA), heme oxygenase-1 (HO-1, 1:100, ab68477, Abcam, Cambridge, MA, USA), NF-κB p65 (1:150, ab16502, Abcam, Cambridge, MA,USA), podocin (1:100, ab50339, Abcam, Cambridge, MA, USA) and vimentin (1:100, ab92547, Abcam, Cambridge, MA, USA) at 4 °C overnight. After incubated with secondary antibody for 2 h at room temperature, slides were incubated with DAPI for 10 min. After mounted with 80% glycerinum in phosphate buffer saline, the slides were subsequently examined by a laser-scanning confocal microscope (FV1000, Olympus Corporation, Tokyo, Japan) equipped with FV10-ASW 4.0 VIEW.

2.10. Western blot analysis

Protein expression was analyzed by western blot. Protein concentration was detected by Pierce™ BCA Protein Assay Kit (23227, Thermo Scientific, New York, New York, USA), and 20–30 μg of total protein was fractionated on 8–12% Tris-Glycine resolving gel at 70 V for 30 min and then 120 V for 60 min. Proteins were transferred to a 0.45 μm PVDF membrane (10600023, Amersham™ Hybond™, GE Healthcare, New York, New York, USA) for 60 min at 230 mA. The membrane was washed three times in 1 × TBS with 0.1% Tween-20. The membranes were incubated for 1 h in 5% non-fat milk blocking buffer. The membranes were incubated overnight at 4 °C in primary antibody. The membrane was washed in TBS with Tween 20 before 2 h incubation in goat anti-rabbit (1:5000, ab6721, Abcam, Cambridge, MA,USA), goat anti-mouse (1:5000, A21010, Abbkine, California, California, USA) and rabbit anti-goat (1:5000, A21110, Abbkine, California, California, USA) secondary antibodies. The membranes were then visualized by Amersham enhanced chemiluminescence prime Western blotting detection reagent (RPN2232, GE Healthcare, New York, New York, USA) in Tanon 6600 Luminescent Imaging Workstation (Tanon Science & Technology Co., Ltd. Shanghai, China). The photographs were captured by autoluminography, and the ratio of proteins was calculated by densitometry using ImageJ software (version 1.48v, NIH, Bethesda, MD, USA). Band densities were normalized by α-tubulin or glyceraldehyde 3-phosphate dehydrogenase (GAPDH) levels. Each protein was repeated three times.

The following primary antibodies were employed (dilution): Gas6 (1:1000, PA5-72882, Thermo Fisher Scientific, New York, New York, USA), Axl (1:2000, ab226927, Abcam, Cambridge, MA, USA), collagen I (1:5000, ab34710, Abcam, Cambridge, MA,USA), α-SMA (1:300, ab7817, Abcam, Cambridge, MA, USA), fibronectin (1:1000, ab2413, Abcam, Cambridge, MA, USA), vimentin (1:200, ab92547, Abcam, Cambridge, MA, USA), E-cadherin (1:500, ab76055, Abcam, Cambridge, MA, USA), fibroblast-specific protein 1 (FSP1, 1:1000, ab197896, Abcam, Cambridge, MA, USA), inhibitor of kappa B alpha (IκBα, 1:2000, 4812, Cell Signaling Technology, USA), phosphorylated-IκBα (p-IκBα, 1:2000, 2859, Cell Signaling Technology, USA), NF-κB p65 (1:2000, ab16502, Abcam, Cambridge, MA, USA), monocyte chemoattractant protein-1 (MCP-1, 1:1000, ab7202, Abcam, Cambridge, MA, USA), cyclooxygenase-2 (COX-2, 1:1000, ab62331, Abcam, Cambridge, MA, USA), Nrf2 (1:1000, ab31163, Abcam, Cambridge, MA,USA), HO-1 (1:2000, ab68477, Abcam, Cambridge, MA, USA), Keap1 (1:250, ab218815, Abcam, Cambridge, MA,USA), catalase (1:1000, ab16731,Abcam, Cambridge, MA, USA), glutamate cysteine ligase catalytic subunit (GCLC, 1:500, ab80841,Abcam, Cambridge, MA, USA), iNOS (1:1000, ab15323, Abcam, Cambridge, MA, USA), 12-lipoxygenase (12-LO, 1:1000, ab211506, Abcam, Cambridge, MA, USA), Ras-related C3 botulinum toxin substrate 1 (Rac1,1:1000, ab33186, Abcam, Cambridge, MA, USA), p^{47phox} (1:1000, ab795, Abcam, Cambridge, MA, USA), p^{67phox} (1:1000, ab109366, Abcam, Cambridge, MA, USA), gp^{91phox} (1:1000, ab31092, Abcam, Cambridge, MA, USA), NAD(P)H quinoneoxidoreductase 1 (NQO-1, ab28947, Abcam, Cambridge, MA, USA), podocin (1:2000, ab50339, Abcam, Cambridge, MA, USA), nephrin (1:1000, ab58968, Abcam, Cambridge, MA, USA), podocalyxin (1:2000, ab154305, Abcam, Cambridge, MA, USA), synaptopodin (1:500, sc-21536, Santa Cruz Biotechnology,

Table 1
Primers for qRT-PCR.

Gene	Forward	Reverse	Product size
IκBα	AGTAACCTACCAGGGCTACTC	ATAGCTCTCCTCATCCTCACTC	133
NF-κB p65	GCTCAAGATCTGCCGAGTAAA	GTCCCGTGAAATACACCTCAA	113
MCP-1	GTCTCAGCCAGATGCAGTTAAT	CTGCTGGTGATTCTCTTGTAGTT	105
COX-2	GGCCATGGAGTGGACTTAAA	GTCTTTGACTGTGGGAGGATAC	132
iNOS	GATATCTTCGGTGCGGTCTTT	TCAGAGTCTTGTGCCTTTGG	78
12-LO	CTCACTCCCTGATGTTCAGAAG	GGTCCTTGGGTCTGAGAAATAC	124
Rac1	CCCACCATTGAGTCCCTTATAG	CTTGTTGGTCAGTGTGAGAGA	102
$p47^{Phox}$	CCCATCATCCTTCAGACCTATC	CTACGACATCCACCACATCTC	97
$p67^{Phox}$	TCGTGTGTTGTTTGGCTTTG	CCAGTTATCACTGCCCTTCTT	97
$gp91^{phox}$	ACCCTCCTATGACTTGGAAATG	TGATGACCACCTTCTGTTGAG	99
Keap1	TCCTCCAGCCCAGTCTTTA	CCGTGTAGGCGAACTCAATTA	124
Nrf2	GGCTAATTGAGTTCGCCTACA	CACGCTGTCAATCTGGTACA	98
HO-1	GATGGCCTCCTTGTACCATATC	AGCTCCTCAGGGAAGTAGAG	99
catalase	CTCAGGTGCGGACATTCTATAC	GACCGCTTTCCTCTGAATGA	116
GCLC	CCTCCTCCTCCAAACTCAGATA	TGGTCAGCAGTACCACAAATAC	112
GPX	CGGGACTACACCGAAATGAA	TCCTGATGTCCGAACTGATTG	95
NQO-1	TGAGAAGAGCCCTGATTGTATTG	CACCTCCCATCCTTTCTTCTTC	104
vimentin	CTTCCCTGAACCTGAGAGAAAC	GTCTCTGGTTTCAACCGTCTTA	98
E-cadherin	GAGGTCTTTGAGGGATCTGTTG	GGCAGCATTGTAGGTGTTTATG	105
collagen I	ACTGGTACATCAGCCCAAAC	GGAACCTTCGCTTCCATACTC	98
α-SMA	AGGGAGTGATGGTTGGAATG	GGTGATGATGCCGTGTTCTA	110
fibronectin	GTGATCTACGAGGGACAGC	GCTGGTGGTGAAGTCAAAG	78
nephrin	CTCAGTGATGACGCAGAGTATG	GGGAAACTAGAATGGAGAGGATTAC	97
podocin	GAGCATTGCCCAAGATGTAAAG	GGCAGCCGTACATCCTTAAT	96
podocalyxin	CTCCATCTCTCTCCCAGGATAA	CATTGCTTGGCTGGTTTGTC	102
synaptopodin	GGTTAGGTCTCCTCCCTCTTAT	CTGTCTTGTTGGCAGGAACTA	95
desmin	TGACTCAGGCAGCCAATAAG	GCATCAATCTCGCAGGTGTA	103
WT1	GGATACAGCACGGTCACTTT	GGTCCTCGTGTTTGAAGGAA	100
ED-1	CTTGGCTCTCTCATTCCCTTAC	TGTATTCCACTGCCATGTAGTT	102
CD3	AGAAAGACAAGATGGCAGAGG	GTGCTGAGACCCTGGTAAAG	97
GAPDH	ACTCCCATTCTTCCACCTTTG	CCCTGTTGCTGTAGCCATATT	105

Dallas, TX, USA), desmin (1:10000, ab32362, Abcam, Cambridge, MA, USA) and Wilms' tumor 1 (WT1, 1:1000, ab180840, Abcam, Cambridge, MA, USA).

2.11. qRT-PCR

Total RNA was isolated from kidneys or NRK-52E cells using a High Pure RNA Isolation Kit (RNAiso Plus, Takara Bio, Otsu, Shiga, Japan). Total RNA (5 μg) was reverse transcribed by Transcriptor First Strand cDNA Synthesis Kit (Roche, Mannheim, Badenia-wirtembergia, Germany). Real-time PCR was performed with SYBR® Premix Ex Taq™ II (Takara Bio, Otsu, Shiga, Japan) using Bio-Rad CFX 96 Touch™ system (Bio-Rad, Hercules, California, USA) for the detection of mRNA expression levels. GAPDH was used as an internal control. The primers used in this study were described in Table 1.

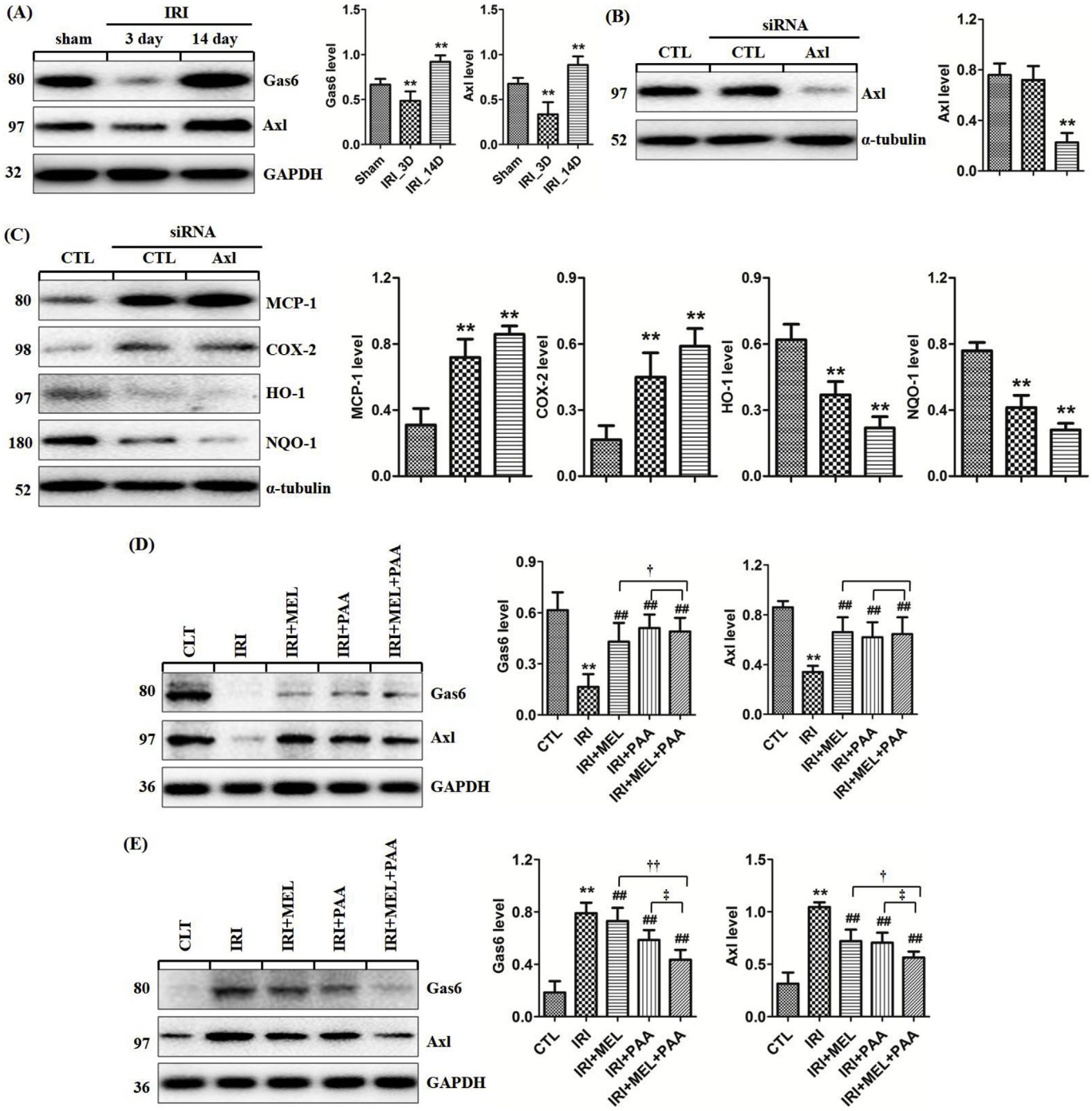

Fig. 2. The different role of Gas6/Axl pathway during AKI-to-CKD transition. (A) The protein levels of Gas6 and Axl in indicated group at days 3 and 14 after IRI procedure. (B) The protein levels of Axl in indicated groups in NRK-52E cells after transfected with Axl RNAi. (C) The protein levels of MCP-1, COX-2, HO-1, and NQO-1 in indicated group in NRK-52E cells after Axl RNAi. (D) The protein levels of Gas6 and Axl in indicated group at day 3 after IRI procedure. (F) The protein levels of Gas6 and Axl in indicated group at day 14 after IRI procedure. Each data represented as the mean ± SD (n = 7). $^{**}p < 0.01$ versus sham or CTL group. $^{\#}p < 0.05$; $^{\#\#}p < 0.01$ versus IRI or H/R group. $^{\dagger}p < 0.05$; $^{\dagger\dagger}p < 0.01$ versus IRI + melatonin or H/R + melatonin group. $^{\ddagger\ddagger}p < 0.01$ versus IRI + PAA group or H/R + PAA group.

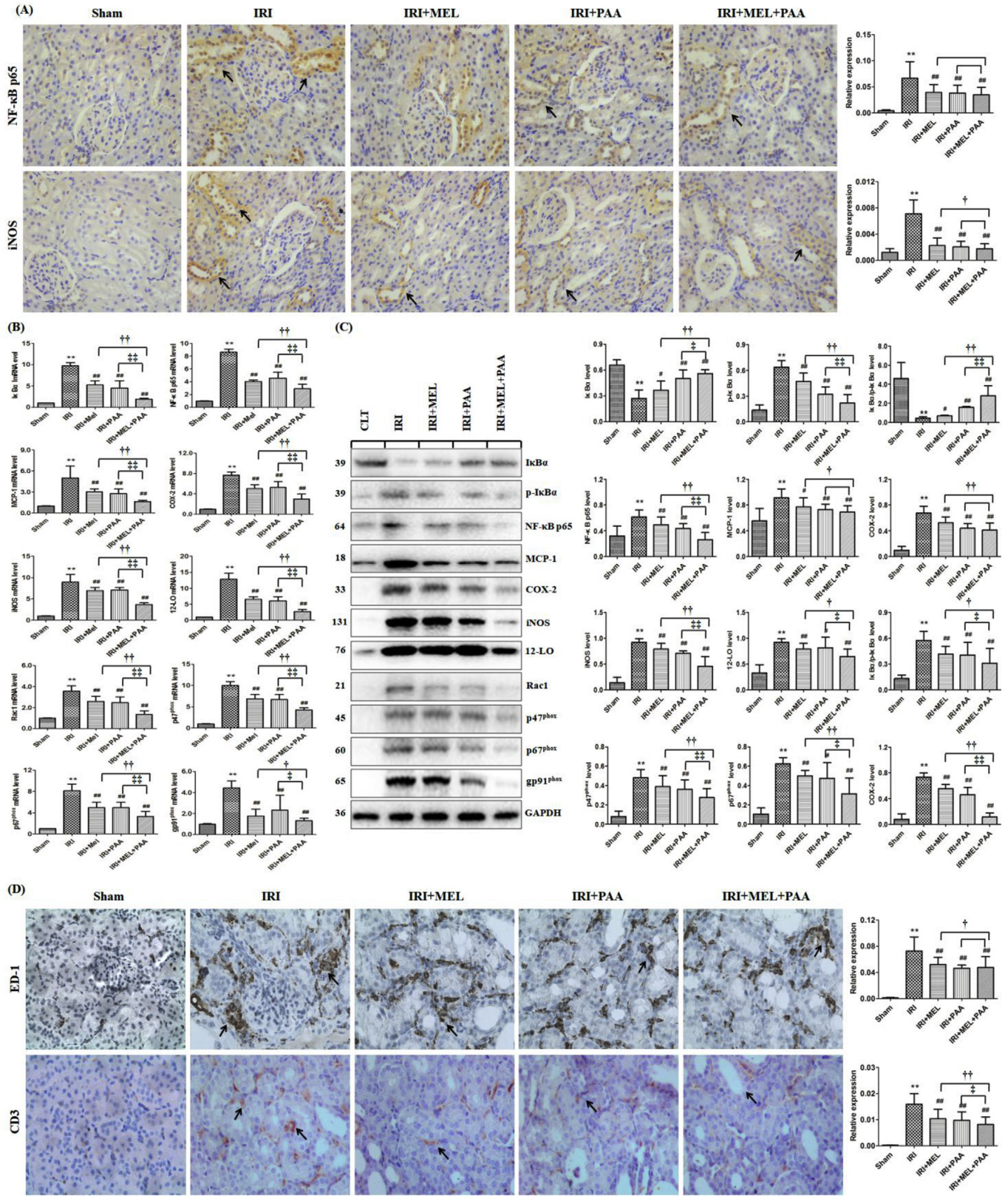

Fig. 3. The inhibitory effects of melatonin and PAA on downstream of Gas6/Axl, NF-κB pathway, in AKI. (A) Representative micrographs of protein expression of NF-κB p65 and iNOS in indicated groups at day 3 after IRI procedure. Arrows indicated positive staining. Magnification, ×400. (B) The mRNA levels of IκBα, NF-κB p65, MCP-1, COX-2, iNOS, 12-LO, rac1, p^{47phox}, p^{67phox}, and gp^{91phox}in indicated groups at day 3 after IRI procedure. (C) The protein levels of IκBα, p-IκBα, p-IκBα/IκBα, NF-κB p65, MCP-1, COX-2, iNOS, 12-LO, rac1, IκBα, p-IκBα, p^{47phox}, p^{67phox}, and gp^{91phox} in indicated groups at day 3 after IRI procedure. (D) Representative micrographs of ED-1 and CD3 protein expression in different groups at day 3 after IRI procedure. Arrows indicated positive staining. Magnification, ×400. Each data represented as the mean ± SD (n = 7). $^{**}p < 0.01$ versus sham group. $^{\#}p < 0.05$; $^{\#\#}p < 0.01$ versus IRI group. $^{\dagger}p < 0.05$; $^{\dagger\dagger}p < 0.01$ versus IRI + melatonin group. $^{\ddagger}p < 0.05$; $^{\ddagger\ddagger}p < 0.01$ versus IRI + PAA group.

2.12. Statistics

The results represented as means ± SD. The statistical analyses were performed using GraphPad Prism software v 5.0 (GraphPad Software, San Diego, CA, USA). The comparisons of multiple groups one-way ANOVA was used followed by Dunnett's *post hoc* test. $p < 0.05$ was considered significant.

3. Results

3.1. The therapeutic effects of melatonin and PAA on IRI rats

Serum creatinine and urea are two important indicators of renal function. As shown in Fig. 1B–C, the levels of serum creatinine and urea were significantly increased at 3 and 14 days in IRI group compared with sham group. Treatment with either melatonin or PAA significantly mitigated the increase levels of serum creatinine and urea. Of note, the combination of melatonin and PAA significantly reduced the levels of serum creatinine and urea at days 3 and 14 in IRI group compared with IRI + melatonin or IRI + PAA group. As shown in Fig. 1D, H&E and masson's trichrome staining of kidney tissues showed edema and loss of renal tubular epithelial cells, tubular dilation, interstitial inflammation and collagen deposition in the kidneys of IRI rats at 14 days. Treatment with melatonin or PAA, especially for combined therapy of melatonin and PAA, significantly ameliorated these lesions.

3.2. The dysregulation of Gas6/Axl in IRI rats during AKI-to-CKD transition

Since Gas6 and its downstream mediator, Axl, exert beneficial effect in IRI in multiple organs at the acute stage and performed pro-fibrotic effects at the chronic stage [8,23], we investigated the expression of Gas6 and Axl. As shown in Fig. 2A, Gas6 and Axl protein expression was significantly downregulated at day 3, but upregulated at day 14 compared with sham group, pointing to different role of Gas6 during AKI-to-CKD transition. As shown in Fig. 2B, Axl protein expression was markedly reduced by specific Axl siRNA in NRK-52E cells. As shown in Fig. 2C, after knock-down of Axl, pro-inflammatory factors MCP-1 and COX-2 were upregulated, while anti-inflammatory factors HO-1 and NQO-1 were downregulated compared with CTL. The inflammation induced by H/R was deteriorated *in vitro* that indicated the anti-inflammatory effects of Axl. Taken together, Gas6/Axl signaling performed anti-inflammatory and anti-fibrotic effects during AKI-to-CKD transition.

Next, we investigated the effects of melatonin and PAA on Gas6/Axl pathway. As shown in Fig. 2D, anti-inflammatory Gas6 and Axl were significantly decreased at 3 days in AKI group. Treatment with melatonin or PAA significantly upregulated the protein expression of Gas6 and Axl compared with IRI rats, indicating that inflammation was attenuated in the kidneys of IRI rats. Of note, combined therapy performed better than single therapy. In CKD, Gas6/Axl pathway is pro-fibrotic route [8]. As shown in Fig. 2E, IRI resulted in the upregulation of Gas6 compared with sham group. Treatment with melatonin or PAA significantly downregulated pro-fibrotic Gas6 protein level, and combined therapy performed better than melatonin or PAA alone. Thus, treatment with melatonin and PAA could favorably regulate Gas6/Axl pathway during AKI-to-CKD transition.

3.3. The regulatory effect of melatonin and PAA on Gas6/Axl–NF–κB pathway in AKI

The upregulation of Gas6 activates its receptor Axl, and Axl activation attenuates inflammation by inhibiting NF-κB pathway in AKI [24]. Since Gas6/Axl pathway could regulate NF-κB pathway, we explored NF-κB pathway in the kidney of IRI rats. NF-κB p65 plays a central role in the activation of NF-κB pathway and IκBα regulates nuclear translocation and DNA binding of NF-κB [25], which is closely related to renal diseases [26–30]. As shown in Fig. 3A, the expression of NF-κB p65 and its target gene iNOS were significantly increased compared with sham rats, while they were decreased after treatment with melatonin or PAA compared with IRI rats. The combined therapy showed stronger inhibitory effects than single therapy. As shown in Fig. 3B–C, significant increase in phosphorylated IκBα and nuclear p65 levels were observed in IRI rats, indicating activation of NF-κB pathway in the kidneys compared with sham rats. This was accompanied by the significant increase in both protein and mRNA levels of targets of NF-κB including MCP-1, COX-2, iNOS and 12-LO and significant increase in NAD(P)H oxidase subunits including Rac1, $p47^{phox}$, $p67^{phox}$ and

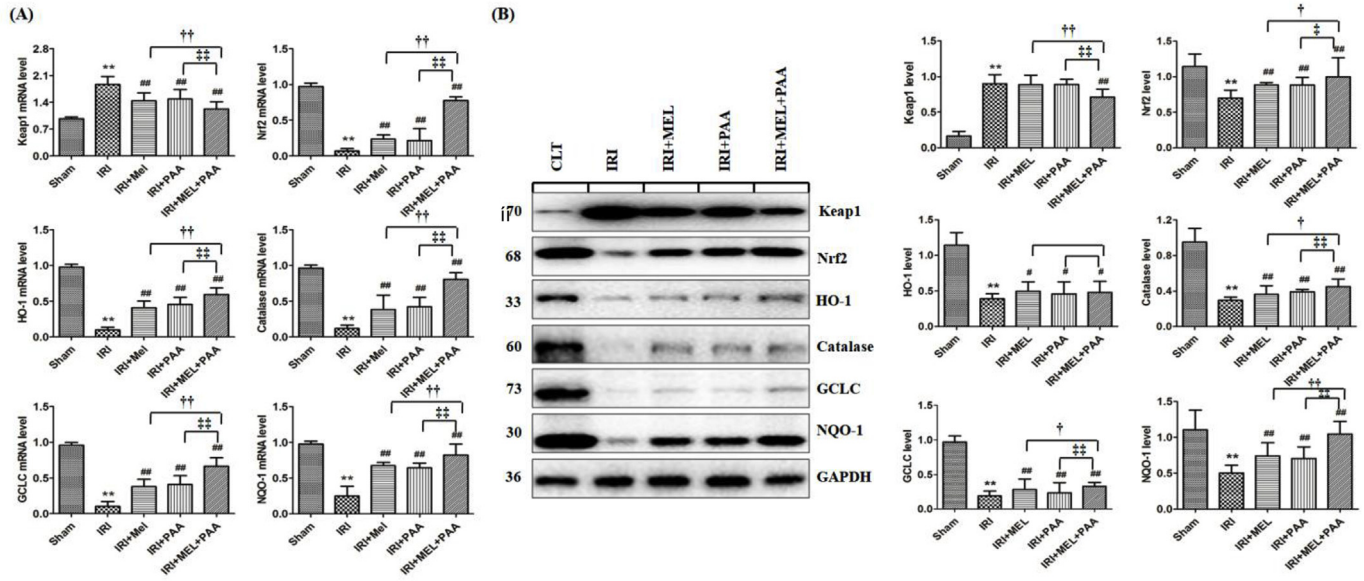

Fig. 4. The regulatory effects of melatonin and PAA on Nrf2 pathway. (A) The mRNA levels of Keap1, Nrf2, HO-1, catalase, GCLC, and NQO-1 in different groups at day 3 after IRI procedure. (B) The protein levels of Keap1, Nrf2, HO-1, catalase, GCLC, and NQO-1 in indicated groups at day 3 after IRI procedure. Each data represented as the mean ± SD (n = 7). $^{**}p < 0.01$ versus sham group. $^{\#}p < 0.05$; $^{\#\#}p < 0.01$ versus IRI group. $^{\dagger}p < 0.05$; $^{\dagger\dagger}p < 0.01$ versus IRI + melatonin group. $^{\ddagger}p < 0.05$; $^{\ddagger\ddagger}p < 0.01$ versus IRI + PAA group.

gp91^{phox} in IRI rats compared with sham rats (Fig. 3B–C). Compared with IRI group, melatonin or PAA treatment significantly ameliorated the activation of NF-κB pathway in IRI rats, and the combined therapy performed better effects than each one alone.

As shown in Fig. 3D, severe interstitial inflammatory infiltration was observed in IRI rats. ED-1 and CD3 are markers of macrophages and T cells, respectively. The overexpression of ED-1 and CD3 in renal interstitium indicated significantly elevated inflammation in the kidneys of IRI rats compared with sham rats. Melatonin or PAA treatment significantly attenuated the expression of ED-1 and CD3 in renal interstitium compared with IRI group. This result demonstrated that melatonin and PAA showed anti-inflammatory effects in IRI rats, and combined therapy performed better than single therapycompared with IRI + melatonin or IRI + PAA group. Therefore, melatonin and PAA could mitigate inflammation through regulating Gas6/Axl−NF−κB pathway in AKI.

3.4. The regulatory effects of melatonin and PAA on Nrf2 pathway in AKI

Nrf2 is a redox regulated transcription factor associated with the regulation of antioxidant defense systems. It promotes the generation of endogenous antioxidant defenses and detoxifying enzymes [31]. Under physiological conditions, there is a balance between Nrf2 and NF-κB pathway. Once an injury occurs, this balance is broken. The deficiency of Nrf2 exacerbates NF-κB activity resulting in increased pro-inflammatory cytokine production, whereas NF-κB modulates Nrf2 transcription and activity [32]. We further explored Nrf2 pathway in AKI stage. Nrf2 is held as an inactive complex in the cytoplasm by the repressor molecule Keap1, which facilitates the ubiquitination of Nrf2 [33]. As shown in Fig. 4, compared with sham rats, a significant reduction in the nuclear Nrf2 level and a significant increase in the Keap1 level were detected in the kidneys of IRI rats. This was accompanied by significant downregulation of Nrf2 target genes including HO-1, catalase, GCLC, and NQO-1 in the kidneys of IRI rats. These findings pointed to the impaired Nrf2 pathway in IRI rats. Treatment with melatonin or PAA mitigated the downregulation of Nrf2 and its downstream targets in IRI rats. Interestingly, combined therapy exerted a stronger activation on Nrf2 pathway than single therapy compared with IRI + melatonin or IRI + PAA group. Taken together, melatonin and PAA performed their anti-inflammatory effects through regulating Gas6/Axl−NF−κB/Nrf2 pathway.

3.5. The inhibition of melatonin and PAA on renal injury through Gas6/Axl pathway in CKD

During AKI-to-CKD transition, increased pro-fibrotic factors cause tubulo-interstitial fibrosis *via* excessive extracellular matrix (ECM) production. The ECM production promotes the process of epithelial-mesenchymal transition (EMT), which has been considered to be a critical process of renal tubulo-interstitial fibrosis. In CKD, Gas6/Axl pathway contributes to fibrogenesis *via* regulation of cell differentiation [8]. As shown in Fig. 2A, Gas6/Axl pathway is reactivated in IRI rats at 14 days, which can stimulate ECM accumulation and accelerate EMT. Collagen I, fibronectin and FSP1 are the components of ECM and promote fibrogenesis though EMT [3]. As shown in Fig. 5A, the results of picro-sirius red stainings showed massive collagen I (red) and collagen III (green) deposition in renal interstitium of IRI rats indicating a serious degree of renal fibrosis at 14 days compared with sham group. Compared with IRI group, melatonin or PAA markedly reduced the deposition of collagen I and collagen III in renal interstitium of CKD rats. As shown in Fig. 5B–C, IRI rats exhibited a significant upregulation of collagen I, fibronectin and FSP1 proteins compared with sham group, while treatment with melatonin or PAA reversed the upregulation of collagen I, fibronectin and FSP1 in IRI rats. Melatonin or PAA treatment also suppressed the expression of markers of mesenchymal cells, α-SMA and vimentin, which were the components of ECM and promoted EMT. Compared with sham rats, IRI rats exhibited a significant downregulation of E-cadherin (a classical epithelial cell marker) at both mRNA and protein levels. Compared with IRI rats, melatonin or PAA treatment reversed the aberrant mRNA and protein levels of α-SMA, vimentin and E-cadherin in IRI rats. Transforming growth factor beta 1 (TGF-β1) plays a dominant role in fibrogenesis [34]. Compared with sham rats, the upregulation of TGF-β1 was observed in renal tubules of IRI rats. Treatment with melatonin or PAA reversed the upregulation of TGF-β1 expression in IRI rats (Fig. 5D).

Podocyte loss induces the depletion of nephrin, podocin, podocalyxin, synaptopodin, and WT1 and the elevation of desmin [35]. Compared with sham rats, the downregulation of nephrin, podocin, podocalyxin, synaptopodin and WT1 as well as the upregulation of desmin were observed in IRI rats (Fig. 5E–F). Compared with IRI rats, treatment with melatonin or PAA significantly reversed these aberrant expression at both mRNA and protein levels in IRI rats. Immunofluorescence staining results also indicated the expression of podocin (green) and E-cadherin (red) were increased by melatonin and PAA treatment (Fig. 5G). Both melatonin and PAA significantly inhibited Gas6/Axl pathway and further suppressed renal fibrosis and podocyte injury, and combined therapy was more effective than single therapy.

3.6. The effects of melatonin and PAA on Gas6/Axl−NF−κB pathway in H/R-induced cell injury

Whether melatonin and PAA exerted their anti-inflammatory effects *via* regulating Gas6/Axl−NF−κB pathway in NRK-52E cells were further explored. First, we examined the proliferative or cytotoxic effects of melatonin and PAA on NRK-52E cells. According to cell viability results shown in Fig. 6A, neither melatonin or PAA caused proliferative or cytotoxic effects at the concentrations of 1, 10, 50 and 100 μM. As shown in Fig. 6B, H/R induced significant decrease of epithelial cell marker E-cadherin at 6 h after H/R compared with CTL group. As shown in Fig. 6C–D, melatonin or PAA reversed the H/R induced fall in E-cadherin expression compared with H/R group. Based on these results, the concentration of 10 μM melatonin and 10 μM PAA were selected for further experiments. As shown in Fig. 2D, inflammation occurred and Gas6/Axl pathway was inhibited after H/R stimulation compared with CTL group, which might result in the activation of NF-κB pathway and further break the balance between NF-κB and Nrf2 pathway. As shown in Fig. 6E–F, the upregulation of p-IκBα and NF-κB p65 and the downregulation of IκBα were observed after H/R, events which were attenuated by melatonin or PAA treatments. Significant increase in NAD(P)H oxidase subunits including Rac1, p47^{phox}, p67^{phox} and gp91^{phox} were upregulated and significant decrease in MCP-1, COX-2, iNOS and 12-LO were downregulated after treatment with melatonin and PAA (Fig. 6E–F). Immunofluorescence staining of NF-κB p65 demonstrated that p65 upregulated and transferred into the nucleus after H/R, but reduced after treatment with melatonin or PAA (Fig. 6G). Consistent with the results *of in vivo experiments*, combined therapy exerted a stronger inhibitory effect on inflammatory pathway than single therapy. Melatonin and PAA activated Gas6/Axl and further inhibited NF-κB to reduce inflammation induced by H/R stimulation.

3.7. The effects of melatonin and PAA on Nrf2 pathway in H/R-induced ***cellular*** injury

Nrf2 signaling pathway after H/R in the present or absent of melatonin and PAA was further detected in NRK-52E cells. As shown in Fig. 7A–B, increased Keap1 and decreased Nrf2 were observed at both mRNA and protein levels in NRK-52E after H/R exposure. The mRNA and protein expression of Nrf2 downstream targets HO-1, catalase, GCLC, and NQO-1 were also significantly decreased after H/R stimulation. Compared with H/R group, melatonin and PAA treatment reactivated Nrf2 signaling and upregulated the expression of downstream

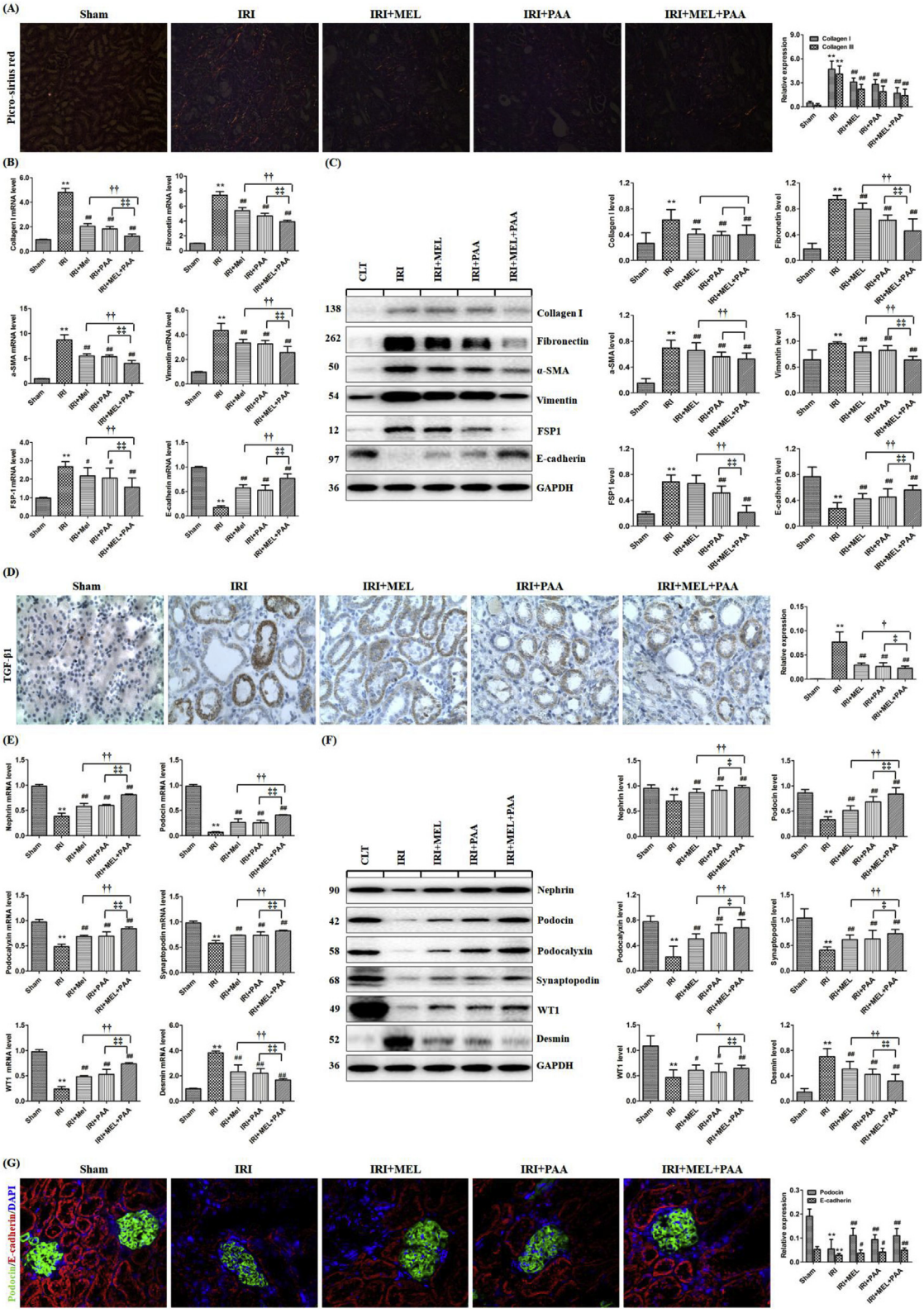

Fig. 5. The anti-fibrotic effects and renoprotective effects of melatonin and PAA in CKD. (A) Representative micrographs of picro-sirius red staining of collagen I (red) and collagen III (green) in indicated groups at day 14 after IRI procedure. Magnification, ×40. (B) The mRNA levels of collagen I, fibronectin, α-SMA, vimentin, FSP1, and E-cadherin in indicated groups at day 14 after IRI procedure. (C) The protein levels of collagen I, fibronectin, α-SMA, vimentin, FSP1, and E-cadherin in indicated groups at day 14 after IRI procedure. (D) Immunohistochemistry staining of TGF-β1 in indicated groups at day 14 after IRI procedure. Arrows indicated positive staining. Magnification, ×400. (E) The mRNA levels of nephrin, podocin, podocalyxin, synaptopodin, WT1, and desmin in indicated groups at day 14 after IRI procedure. (F) The protein levels of nephrin, podocin, podocalyxin, synaptopodin, WT1, and desmin in indicated groups at day 14 after IRI procedure. (G) Immunofluorescence staining of podocin (green) and E-cadherin (red) in indicated groups at day 14 after IRI procedure. Magnification, ×400. Each data represented as the mean ± SD (n = 7). $^{**}p < 0.01$ versus sham group. $^{\#}p < 0.05$; $^{\#\#}p < 0.01$ versus IRI group. $^{\dagger}p < 0.05$; $^{\dagger\dagger}p < 0.01$ versus IRI + melatonin group. $^{\ddagger}p < 0.05$; $^{\ddagger\ddagger}p < 0.01$ versus IRI + PAA group. (For interpretation of the references to colour in this figure legend, the reader is referred to the Web version of this article.)

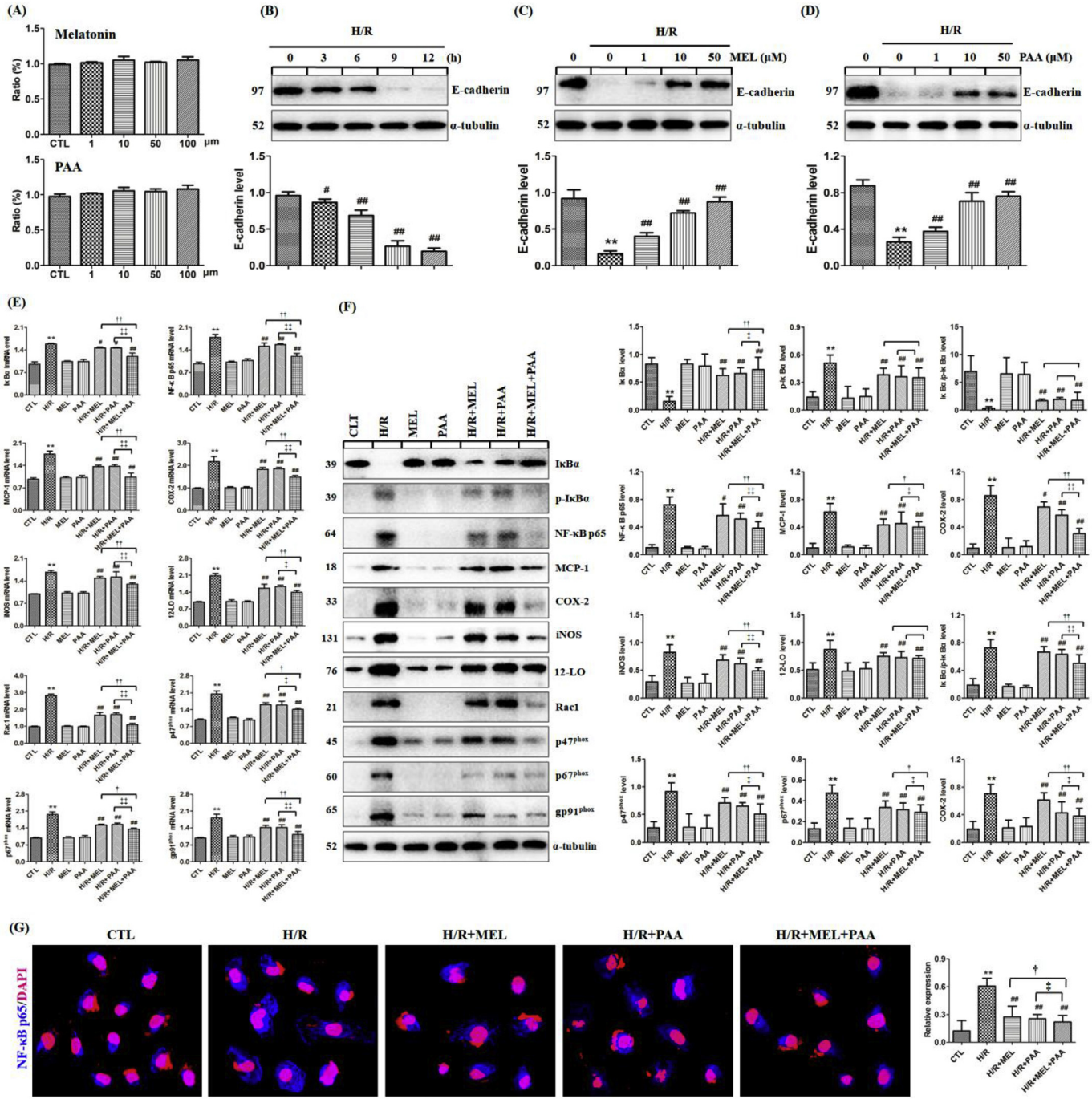

Fig. 6. The inhibition of melatonin and PAA on downstream of Gas6/Axl, NF-κB pathway, in H/R-induced NRK-52E cells. (A) The cell viabilities of NRK-52E cells after incubation with melatonin or PAA for 24 h. (B) E-cadherin protein expression in different hypoxia time following reoxygenation for 12 h. (C) E-cadherin protein expression after H/R (melatonin was added in reoxygenation). (D) E-cadherin protein expression after H/R (PAA was added in reoxygenation). (E) The mRNA levels of IκBα, NF-κB p65, MCP-1, COX-2, iNOS, 12-LO, rac1, p^{47phox}, p^{67phox}, and gp^{91phox} in indicated groups after hypoxia for 9 h following reoxygenation for 6 h. (F) The protein levels of IκBα, p-IκBα, NF-κB p65, MCP-1, COX-2, iNOS, 12-LO, rac1, p^{47phox}, p^{67phox}, and gp^{91phox}. (G) Immunofluorescence staining of NF-κB p65 (blue) in indicated groups. Magnification, ×800. Each data represented as the mean ± SD. $^{**}p < 0.01$ versus CTL group. $^{\#}p < 0.05$; $^{\#\#}p < 0.01$ versus H/R group. $^{\dagger}p < 0.05$; $^{\dagger\dagger}p < 0.01$ versus H/R + melatonin group. $^{\ddagger}p < 0.05$; $^{\ddagger\ddagger}p < 0.01$ versus H/R + PAA group. (For interpretation of the references to colour in this figure legend, the reader is referred to the Web version of this article.)

targets. Immunofluorescence staining of HO-1 indicated that the downregulation of HO-1 induced by H/R was upregulated after melatonin and PAA treatment (Fig. 7C). Compared with H/R + melatonin or H/R + PAA group, the combined therapy exhibited better in activating Nrf2 signaling. Therefore, melatonin and PAA exerted anti-inflammatory effects by regulating Gas6/Axl−NF−κB/Nrf2 pathway *in vitro*.

4. Discussion

Renal IRI results in the dysfunction and damage in renal tubules, interstitium and glomeruli [36]. Renal IRI is a common route of AKI to CKD and renal fibrosis [3]. During AKI-to-CKD transition, oxidative stress and inflammation subsequently contributes to post-ischemic fibrosis [37,38]. Owing to such a complex pathogenesis, the use of single

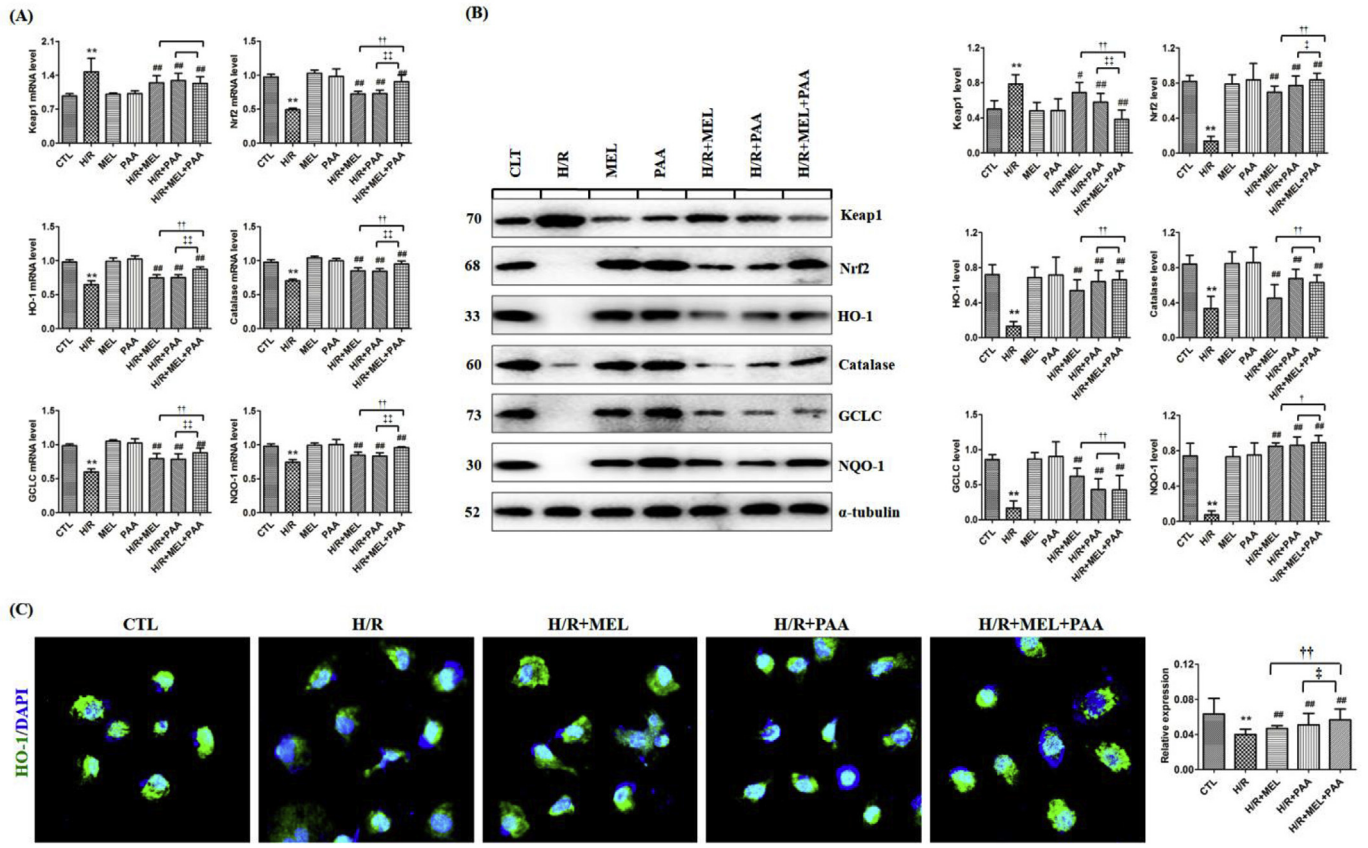

Fig. 7. The regulatory effects of melatonin and PAA on Nrf2 pathway in H/R-induced NRK-52E cells. (A) The mRNA levels of Keap1, Nrf2, HO-1, catalase, GCLC, and NQO-1 in indicated groups after hypoxia for 9 h following reoxygenation for 6 h. (B) The protein levels of Keap1, Nrf2, HO-1, catalase, GCLC, and NQO-1 in indicated groups. (C) Immunofluorescence staining of HO-1 (green) in indicated groups. Magnification, ×800. Each data represented as the mean ± SD. $^{**}p < 0.01$ versus CTL group. $^{\#}p < 0.05$; $^{\#\#}p < 0.01$ versus H/R group. $^{\dagger}p < 0.05$; $^{\dagger\dagger}p < 0.01$ versus H/R + melatonin group. $^{\ddagger}p < 0.05$; $^{\ddagger\ddagger}p < 0.01$ versus H/R + PAA group. (For interpretation of the references to colour in this figure legend, the reader is referred to the Web version of this article.)

agent for simultaneously modifying multiple targets is not completely effective in the treatment of IRI and preventing AKI-to-CKD transition. Therefore, developing a combination therapy to simultaneously target multiple pathways is necessary for the effective treatment of IRI and the blockage of AKI-to-CKD transition. Our results demonstrated that, during AKI-to-CKD transition, treatment with melatonin and PAA ameliorated oxidative stress and inflammation, and mitigated renal fibrosis *via* regulating Gas6/Axl−NF−κB/Nrf2 pathway (Fig. 8).

Natural products have long been used in clinical practice and have been considered an alternative therapy for the prevention and treatment of various renal diseases [13,39–41]. Mounting evidence has suggested that many small molecular compounds extracted from natural products exerted their anti-fibrotic effects by improving the dysregulation of renin-angiotensin system (RAS), oxidative stress and inflammation, TGF-β/Smad and Wnt/β-catenin signaling pathways as well as the dysregulation of uremic toxins, amino acid and lipid metabolism [29,42–47]. In this study, PAA treatment significantly lowered creatinine and urea levels and retarded AKI-to-CKD transition indicating its renoprotective effects. Our latest studies demonstrated that several poricoic acids could protect against renal fibrosis by inhibiting RAS activation and TGF-β/Smad and Wnt/β-catenin pathways in both *in vitro* and *in vivo* experiments [48–50]. Another study demonstrated that dehydroeburicoic acid monoacetate isolated from *Poria cocos* could inhibit cisplatin-induced nephrotoxicity by inhibiting the upregulated expression of phosphorylation of the mitogen-activated protein kinase, c-Jun N-terminal kinase, extracellular signal-regulated kinase, and p38 and caspase-3 in the kidney proximal tubule cells (LLC-PK1) [51]. Due to the similar chemical structures among these components isolated from *P. cocos,* these previous studies supported renoprotective effect of PAA by retarding AKI-to-CKD transition. Similar results were also observed by melatonin treatment during AKI-to-CKD transition. Intriguingly, PAA could enhance the inhibitory effect of melatonin on AKI-to-CKD transition.

Melatonin is one of the metabolites of tryptophan. Tryptophan hydroxylase-2 converts L-tryptophan to 5-hydroxytryptophan (5-HTP), which is a key intermediate metabolite of the biosynthesis of serotonin and melatonin [52]. 5-HTP is then converted to serotonin by aromatic amino acid decarboxylase [53]. The metabolite of L-tryptophan, 5-methoxyindole, inhibited COX-2 expression at the transcriptional level. 5-HTP inhibited COX-2 expression through conversion to 5-methoxytryptophan (5-MTP) [52]. Based on metabolomic analysis, several studies have demostrated the metabolism disorders of various amino acid in animal models of AKI and CKD [54–58]. The significantly aberrant tryptophan level has extensively demonstrated in both animal models and patients with AKI or CKD [58–64]. In addition, the levels of 5-HTP and 5-MTP are significantly altered in AKI mice and CKD patients, respectively [27,58]. Our previous study suggested that SLPC extract could protect against renal fibrosis and improve the abnormal serum tryptophan level in adenine-induced CKD rats [65]. Therefore, these data strongly supported that synergetic effect of PAA and melatonin in retarding AKI-to-CKD transition might be partially associated with their effect on tryptophan metabolism.

To explore the mechanisms by which PAA and melatonin retarded renal injury, we examined their effects on Gas6/Axl−NF−κB/Nrf2 signaling cascade. Gas6 is a vitamin K-dependent protein and shows anti-inflammatory effects [66]. Gas6 dampens acute inflammation through stimulation of its downstream mediators, a family of receptor tyrosine kinase receptors, including Tyro3, Axl and MerTK [8]. Among the three

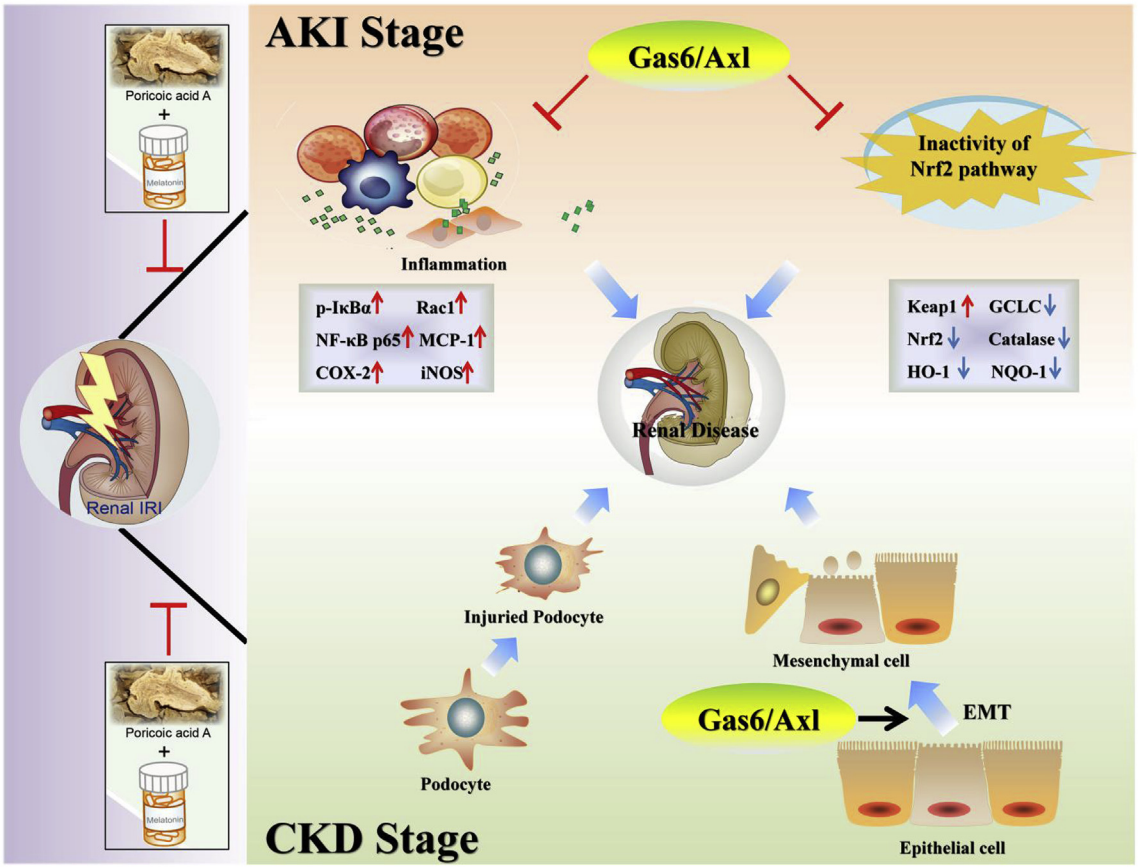

Fig. 8. Schematic diagram depicting possible mechanisms involved in protective effects of melatonin and PAA during AKI-to-CKD transition. During AKI period, melatonin and PAA alleviated inflammation and improved renal injury through activating anti-inflammatory Gas6/Axl and Nrf2 pahways, and inhibiting pro-inflammatory NF-κB pathway. During CKD period, melatonin and PAA retarded podocyte injury and inhibited EMT through suppressing pro-fibrotic Gas6/Axl pathway.

receptors, Axl receptor has the greatest affinity for Gas6 and performs its anti-inflammatory effects *via* regulating NF-κB and NADPH oxidase [8]. In the present study, we found that knock-down of Axl contributes to inflammation, which was consistent with previous study [67]. During AKI-to-CKD transition, the role of Gas6/Axl is opposite. The activation of Gas6/Axl is anti-inflammatory in AKI, while Gas6/Axl is pro-fibrotic in CKD. Our present study showed that melatonin or PAA administration inhibited upregulation of Gas6/Axl pathway at day 3 and downregulated Gas6/Axl pathway during AKI-to-CKD transition.. Combined therapy exerted strongly regulatory effects on Gas6/Axl pathway during AKI-to-CKD transition.

Oxidative stress and inflammation are inseparably linked as they form a vicious cycle [6]. Our present results demonstrated that PAA and melatonin treatment ameliorated oxidative stress and inflammation during AKI-to-CKD transition. As the downstream of Gas6/Axl pathway, NF-κB signaling pathway plays a dominant role in accelerating oxidative stress and inflammation after IRI. The activation of NF-κB pathway affects Nrf2 pathway that controls cellular oxidative stress and inflammatory response. The Nrf2 pathway is the most pivotal endogenous antioxidative system [68], and the balance between NF-κB and Nrf2 controls oxidative stress and inflammation. Previous studies demonstrated that pro-inflammatory cytokines and macrophage infiltration contributed to the renal IRI [69]. Mounting evidence has demonstrated that oxidative stress and inflammation played a central role in the pathogenesis and progression of CKD [70,71]. Our present findings demonstrated that both melatonin and PAA significantly activated Gas6/Axl pathway and further inhibited the activation of NF-κB pathway and activated Nrf2 pathway in IRI rats and H/R treated cells. Our recent study demonstrated pachymic acid B from *P. cocos* could inhibit upregulation of NF-κB and inflammatory genes including MCP-1 and COX-2 expression as well as increase the downregulation of antioxidant system including Nrf2 and HO-1 expression in angiotensin II-induced human kidney proximal epithelial cells (HK-2) [34]. Extensive evidence has demonstrated that melatonin exerted its renoprotective effect by improving oxidative stress and inflammation [72]. These finding supported the enhanced protection of combined PAA and melatonin against renal IRI in a rodent model. One possible explanation is that melatonin mainly localizes in a superficial position on the lipid bilayers near the polar heads of the membrane phospholipids when it enters cellular membranes. While in this position, melatonin is capable of functioning as a free radical scavenger and may also provide an indirect means by which the membranes resist oxidative damage [73]. Interestingly, previous study reported that renal IRI insignificantly elevated the plasma total antioxidant capacity, which was explained as a cellular defensive response to overproduction of reactive oxygen species after renal IRI [74].

In conclusion, our study demonstrated that melatonin and PAA exhibited renoprotective effects during AKI-to-CKD transition by the regulation of Gas6/Axl−NF−κB/Nrf2 pathway. Notably, the synergetic enhancement of melatonin and PAA protected against renal IRI more effectively than either drug alone. Our study first found that Axl is a promising therapeutic target in AKI-to-CKD transition, which provides new candidates and strategies for the treatment of renal disease.

Conflicts of interest

The authors have declared that no competing interest exists.

Acknowledgments

This study was supported by the National Natural Science Foundation of China (Nos. 81872985, 81673578).

References

[1] A. Zuk, J.V. Bonventre, Acute kidney injury, Annu. Rev. Med. 67 (2016) 293–307.
[2] L.S. Chawla, P.W. Eggers, R.A. Star, P.L. Kimmel, Acute kidney injury and chronic kidney disease as interconnected syndromes, N. Engl. J. Med. 371 (1) (2014) 58–66.
[3] L. Xiao, D. Zhou, R.J. Tan, H. Fu, L. Zhou, F.F. Hou, Y. Liu, Sustained activation of Wnt/β-catenin signaling drives AKI to CKD progression, J. Am. Soc. Nephrol. 27 (6) (2016) 1727–1740.
[4] M. Shuvy, S. Abedat, R. Beeri, M. Valitsky, S. Daher, M. Kott-Gutkowski, A. Gal-Moscovici, J. Sosna, N.M. Rajamannan, C. Lotan, Raloxifene attenuates Gas6 and apoptosis in experimental aortic valve disease in renal failure, Am. J. Physiol. Heart Circ. Physiol. 300 (5) (2011) H1829–H1840.
[5] L. Llacuna, C. Barcena, L. Bellido-Martin, L. Fernandez, M. Stefanovic, M. Mari, C. Garcia-Ruiz, J.C. Fernandez-Checa, P. Garcia de Frutos, A. Morales, Growth arrest-specific protein 6 is hepatoprotective against murine ischemia/reperfusion injury, Hepatology 52 (4) (2010) 1371–1379.
[6] S. Ruiz, P.E. Pergola, R.A. Zager, N.D. Vaziri, Targeting the transcription factor Nrf2 to ameliorate oxidative stress and inflammation in chronic kidney disease, Kidney Int. 83 (6) (2013) 1029–1041.
[7] L. He, Q. Wei, J. Liu, M. Yi, Y. Liu, H. Liu, L. Sun, Y. Peng, F. Liu, M.A. Venkatachalam, Z. Dong, AKI on CKD: heightened injury, suppressed repair, and the underlying mechanisms, Kidney Int. 92 (5) (2017) 1071–1083.
[8] C. Barcena, M. Stefanovic, A. Tutusaus, L. Joannas, A. Menendez, C. Garcia-Ruiz, P. Sancho-Bru, M. Mari, J. Caballeria, C.V. Rothlin, J.C. Fernandez-Checa, P.G. de Frutos, A. Morales, Gas6/Axl pathway is activated in chronic liver disease and its targeting reduces fibrosis via hepatic stellate cell inactivation, J. Hepatol. 63 (3) (2015) 670–678.
[9] B.C. Koch, K. van der Putten, E.J. Van Someren, J.P. Wielders, P.M. Ter Wee, J.E. Nagtegaal, C.A. Gaillard, Impairment of endogenous melatonin rhythm is related to the degree of chronic kidney disease (CREAM study), Nephrol. Dial. Transplant. 25 (2) (2010) 513–519.
[10] D. Atilgan, B.S. Parlaktas, N. Uluocak, F. Erdemir, F. Firat, U. Erkorkmaz, O. Saylan, Effects of melatonin on partial unilateral ureteral obstruction induced oxidative injury in rat kidney, Urol. Ann. 4 (2) (2012) 89–93.
[11] K.H. Chen, C.H. Chen, C.G. Wallace, Y.T. Chen, C.C. Yang, P.H. Sung, H.J. Chiang, Y.L. Chen, S. Chua, H.K. Yip, J.T. Cheng, Combined therapy with melatonin and exendin-4 effectively attenuated the deterioration of renal function in rat cardiorenal syndrome, Am. J. Transl. Res. 9 (2) (2017) 214–229.
[12] D. Shen, X. Tian, W. Sang, R. Song, Effect of Melatonin and Resveratrol against memory impairment and hippocampal damage in a rat model of vascular dementia, Neuroimmunomodulation 23 (5–6) (2016) 318–331.
[13] D.Q. Chen, Y.L. Feng, G. Cao, Y.Y. Zhao, Natural products as a source for anti-fibrosis therapy, Trends Pharmacol. Sci. 39 (11) (2018) 937–952.
[14] D.Q. Chen, H.H. Hu, Y.N. Wang, Y.L. Feng, G. Cao, Y.Y. Zhao, Natural products for the prevention and treatment of kidney disease, Phytomedicine 50 (2018) 50–60.
[15] L. Chen, T. Yang, D.W. Lu, H. Zhao, Y.L. Feng, H. Chen, D.Q. Chen, N.D. Vaziri, Y.Y. Zhao, Central role of dysregulation of TGF-β/Smad in CKD progression and potential targets of its treatment, Biomed. Pharma 101 (2018) 670–681.
[16] Y.Z. Wang, J. Zhang, Y.L. Zhao, T. Li, T. Shen, J.Q. Li, W.Y. Li, H.G. Liu, Mycology, cultivation, traditional uses, phytochemistry and pharmacology of Wolfiporia cocos (Schwein.) Ryvarden et Gilb.: a review, J. Ethnopharmacol. 147 (2) (2013) 265–276.
[17] Y.L. Feng, P. Lei, T. Tian, L. Yin, D.Q. Chen, H. Chen, Q. Mei, Y.Y. Zhao, R.C. Lin, Diuretic activity of some fractions of the epidermis of Poria cocos, J. Ethnopharmacol. 150 (3) (2013) 1114–1118.
[18] Y.Y. Zhao, Y.L. Feng, X. Du, Z.H. Xi, X.L. Cheng, F. Wei, Diuretic activity of the ethanol and aqueous extracts of the surface layer of *Poria cocos* in rat, J. Ethnopharmacol. 144 (3) (2012) 775–778.
[19] Y.Y. Zhao, P. Lei, D.Q. Chen, Y.L. Feng, X. Bai, Renal metabolic profiling of early renal injury and renoprotective effects of *Poria cocos* epidermis using UPLC Q-TOF/HSMS/MS^{E}, J. Pharmaceut. Biomed. Anal. 81 (82) (2013) 202–209.
[20] Y.Y. Zhao, H.T. Li, Y.I. Feng, X. Bai, R.C. Lin, Urinary metabonomic study of the surface layer of *Poria cocos* as an effective treatment for chronic renal injury in rats, J. Ethnopharmacol. 148 (2) (2013) 403–410.
[21] H.K. Yip, C.C. Yang, K.H. Chen, T.H. Huang, Y.L. Chen, Y.Y. Zhen, P.H. Sung, H.J. Chiang, J.J. Sheu, C.L. Chang, C.H. Chen, H.W. Chang, Y.T. Chen, Combined melatonin and exendin-4 therapy preserves renal ultrastructural integrity after ischemia-reperfusion injury in the male rat, J. Pineal Res. 59 (4) (2015) 434–447.
[22] Z.H. Zhang, N.D. Vaziri, F. Wei, X.L. Cheng, X. Bai, Y.Y. Zhao, An integrated lipidomics and metabolomics reveal nephroprotective effect and biochemical mechanism of *Rheum officinale* in chronic renal failure, Sci. Rep. 6 (2016) 22151.
[23] L.W. Chen, W. Chen, Z.Q. Hu, J.L. Bian, L. Ying, G.L. Hong, Q.M. Qiu, G.J. Zhao, Z.Q. Lu, Protective effects of growth arrest-specific protein 6 (Gas6) on sepsis-induced acute kidney injury, Inflammation 39 (2) (2016) 575–582.
[24] G. Wu, D.W. McBride, J.H. Zhang, Axl activation attenuates neuroinflammation by inhibiting the TLR/TRAF/NF-κB pathway after MCAO in rats, Neurobiol. Dis. 110 (2018) 59–67.
[25] A.B. Sanz, M.D. Sanchez-Nino, A.M. Ramos, J.A. Moreno, B. Santamaria, M. Ruiz-Ortega, J. Egido, A. Ortiz, NF-κB in renal inflammation, J. Am. Soc. Nephrol. 21 (8) (2010) 1254–1262.
[26] J. Chen, I.L. Leskov, A. Yurdagul Jr., B. Thiel, C.G. Kevil, K.Y. Stokes, A.W. Orr, Recruitment of the adaptor protein Nck to PECAM-1 couples oxidative stress to canonical NF-κB signaling and inflammation, Sci. Signal. 8 (365) (2015) ra20.
[27] D.Q. Chen, G. Cao, H. Chen, D. Liu, W. Su, X.Y. Yu, N.D. Vaziri, X.H. Liu, X. Bai, L. Zhang, Y.Y. Zhao, Gene and protein expressions and metabolomics exhibit activated redox signaling and wnt/β-catenin pathway are associated with metabolite dysfunction in patients with chronic kidney disease, Redox Biol 12 (2017) 505–521.
[28] D.Q. Chen, H. Chen, L. Chen, N.D. Vaziri, M. Wang, X.R. Li, Y.Y. Zhao, The link between phenotype and fatty acid metabolism in advanced chronic kidney disease, Nephrol. Dial. Transplant. 32 (7) (2017) 1154–1166.
[29] H. Chen, G. Cao, D.Q. Chen, M. Wang, N.D. Vaziri, Z.H. Zhang, J.R. Mao, X. Bai, Y.Y. Zhao, Metabolomics insights into activated redox signaling and lipid metabolism dysfunction in chronic kidney disease progression, Redox Biol 10 (2016) 168–178.
[30] Y.Y. Zhao, H.L. Wang, X.L. Cheng, F. Wei, X. Bai, R.C. Lin, N.D. Vaziri, Metabolomics analysis reveals the association between lipid abnormalities and oxidative stress, inflammation, fibrosis, and Nrf2 dysfunction in aristolochic acid-induced nephropathy, Sci. Rep. 5 (2015) 12936.
[31] V. Ganesh Yerra, G. Negi, S.S. Sharma, A. Kumar, Potential therapeutic effects of the simultaneous targeting of the Nrf2 and NF-κB pathways in diabetic neuropathy, Redox Biol 1 (2013) 394–397.
[32] J.D. Wardyn, A.H. Ponsford, C.M. Sanderson, Dissecting molecular cross-talk between Nrf2 and NF-κB response pathways, Biochem. Soc. Trans. 43 (4) (2015) 621–626.
[33] E. Kansanen, S.M. Kuosmanen, H. Leinonen, A.L. Levonen, The Keap1-Nrf2 pathway: mechanisms of activation and dysregulation in cancer, Redox Biol 1 (2013) 45–49.
[34] L. Chen, D.Q. Chen, M. Wang, D. Liu, H. Chen, F. Dou, N.D. Vaziri, Y.Y. Zhao, Role of RAS/Wnt/β-catenin axis activation in the pathogenesis of podocyte injury and tubulo-interstitial nephropathy, Chem. Biol. Interact. 273 (2017) 56–72.
[35] L. Zhou, Y. Li, S. Hao, D. Zhou, R.J. Tan, J. Nie, F.F. Hou, M. Kahn, Y. Liu, Multiple genes of the renin-angiotensin system are novel targets of Wnt/β-catenin signaling, J. Am. Soc. Nephrol. 26 (1) (2015) 107–120.
[36] M.S. Paller, Acute renal failure: controversies, clinical trials, and future directions, Semin. Nephrol. 18 (5) (1998) 482–489.
[37] S.G. Coca, B. Yusuf, M.G. Shlipak, A.X. Garg, C.R. Parikh, Long-term risk of mortality and other adverse outcomes after acute kidney injury: a systematic review and meta-analysis, Am. J. Kidney Dis. 53 (6) (2009) 961–973.
[38] M.A. Venkatachalam, K.A. Griffin, R. Lan, H. Geng, P. Saikumar, A.K. Bidani, Acute kidney injury: a springboard for progression in chronic kidney disease, Am. J. Physiol. Renal. Physiol. 298 (5) (2010) F1078–F1094.
[39] Y.Y. Zhao, Traditional uses, phytochemistry, pharmacology, pharmacokinetics and quality control of *Polyporus umbellatus* (Pers.) Fries: a review, J. Ethnopharmacol. 149 (1) (2013) 35–48.
[40] T. Tian, H. Chen, Y.Y. Zhao, Traditional uses, phytochemistry, pharmacology, toxicology and quality control of *Alisma orientale* (Sam.) Juzep: a review, J. Ethnopharmacol. 158 (2014) 373–387.
[41] Z.H. Zhang, F. Wei, N.D. Vaziri, X.L. Cheng, X. Bai, R.C. Lin, Y.Y. Zhao, Metabolomics insights into chronic kidney disease and modulatory effect of rhubarb against tubulointerstitial fibrosis, Sci. Rep. 5 (5) (2015) 14472.
[42] H. Chen, T. Yang, M.C. Wang, D.Q. Chen, Y. Yang, Y.Y. Zhao, Novel RAS inhibitor 25-O-methylalisol F attenuates epithelial-to-mesenchymal transition and tubulo-interstitial fibrosis by selectively inhibiting TGF-β-mediated Smad3 phosphorylation, Phytomedicine 42 (2018) 207–218.
[43] Y.Y. Zhao, L. Zhang, J.R. Mao, X.H. Cheng, R.C. L, Y. Zhang, W.J. Sun, Ergosta-4,6,8(14),22-tetraen-3-one isolated from *Polyporus umbellatus* prevents early renal injury in aristolochic acid-induced nephropathy rats, J. Pharm. Pharmacol. 63 (12) (2011) 1581–1586.
[44] Y.Y. Zhao, X.L. Cheng, J.H. Cui, X.R. Yan, F. Wei, X. Bai, R.C. Lin, Effect of ergosta-4,6,8(14),22-tetraen-3-one (ergone) on adenine-induced chronic renal failure rat: a serum metabonomic study based on ultra performance liquid chromatography/high-sensitivity mass spectrometry coupled with MassLynx i-FIT algorithm, Clin. Chim. Acta 413 (19–20) (2012) 1438–1445.
[45] Y.Y. Zhao, X. Shen, X.L. Cheng, F. Wei, X. Bai, R.C. Lin, Urinary metabonomics study on the protective effects of ergosta-4,6,8(14),22-tetraen-3-one on chronic renal failure in rats using UPLC Q-TOF/MS and a novel MS^{E} data collection technique, Process Biochem. 47 (12) (2012) 1980–1987.
[46] Y.Y. Zhao, H. Chen, T. Tian, D.Q. Chen, X. Bai, F. Wei, A pharmaco-metabonomic study on chronic kidney disease and therapeutic effect of ergone by UPLC-QTOF/HDMS, PLoS One 23 (9) (2014) e115467.
[47] Y.Y. Zhao, L. Zhang, F.Y. Long, X.L. Cheng, X. Bai, F. Wei, R.C. Lin, UPLC-Q-TOF/HSMS/MS^{E}-based metabonomics for adenine-induced changes in metabolic profiles of rat faeces and intervention effects of ergosta-4,6,8(14),22-tetraen-3-one, Chem. Biol. Interact. 201 (1–3) (2013) 31–38.
[48] M. Wang, D.Q. Chen, L. Chen, G. Cao, H. Zhao, D. Liu, N.D. Vaziri, Y. Guo, Y.Y. Zhao, Novel inhibitors of the cellular renin-angiotensin system components, poricoic acids, target Smad3 phosphorylation and Wnt/β-catenin pathway against renal fibrosis, Br. J. Pharmacol. 175 (13) (2018) 2689–2708.
[49] M. Wang, D.Q. Chen, L. Chen, H. Zhao, D. Liu, Z.H. Zhang, N.D. Vaziri, Y. Guo, Y.Y. Zhao, G. Cao, Novel RAS inhibitors poricoic acid ZG and poricoic acid ZH attenuate renal fibrosis via Wnt/β-catenin pathway and targeted phosphorylation of smad3 signaling, J. Agric. Food Chem. 66 (8) (2018) 1828–1842.
[50] M. Wang, D.Q. Chen, M.C. Wang, H. Chen, L. Chen, D. Liu, H. Zhao, Y.Y. Zhao, Poricoic acid ZA, a novel RAS inhibitor, attenuates tubulo-interstitial fibrosis and podocyte injury by inhibiting TGF-β/Smad signaling pathway, Phytomedicine 36

(2017) 243–253.
[51] D. Lee, S. Lee, S.H. Shim, H.J. Lee, Y. Choi, T.S. Jang, K.H. Kim, K.S. Kang, Protective effect of lanostane triterpenoids from the sclerotia of *Poria cocos* Wolf against cisplatin-induced apoptosis in LLC-PK1 cells, Bioorg. Med. Chem. Lett 27 (13) (2017) 2881–2885.
[52] K.K. Wu, H.H. Cheng, T.C. Chang, 5-methoxyindole metabolites of L-tryptophan: control of COX-2 expression, inflammation and tumorigenesis, J. Biomed. Sci. 21 (2014) 17.
[53] J. Best, H.F. Nijhout, M. Reed, Serotonin synthesis, release and reuptake in terminals: a mathematical model, Theor. Biol. Med. Model. 7 (2010) 34.
[54] Y.Y. Zhao, R.C. Lin, Metabolomics in nephrotoxicity, Adv. Clin. Chem. 65 (2014) 69–89.
[55] Z.H. Zhang, H. Chen, N.D. Vaziri, J.R. Mao, L. Zhang, X. Bai, Y.Y. Zhao, Metabolomic signatures of chronic kidney disease of diverse etiologies in the rats and humans, J. Proteome Res. 15 (10) (2016) 3802–3812.
[56] Z.H. Zhang, J.Q. He, W.W. Qin, Y.Y. Zhao, N.H. Tan, Biomarkers of obstructive nephropathy using a metabolomics approach in rat, Chem. Biol. Interact. 296 (2018) 229–239.
[57] Y.Y. Zhao, D.D. Tang, H. Chen, J.R. Mao, X. Bai, X.H. Cheng, X.Y. Xiao, Urinary metabolomics and biomarkers of aristolochic acid nephrotoxicity by UPLC-QTOF/HDMS, Bioanalysis 7 (6) (2015) 685–700.
[58] J.R. Zgoda-Pols, S. Chowdhury, M. Wirth, M.V. Milburn, D.C. Alexander, K.B. Alton, Metabolomics analysis reveals elevation of 3-indoxyl sulfate in plasma and brain during chemically-induced acute kidney injury in mice: investigation of nicotinic acid receptor agonists, Toxicol. Appl. Pharmacol. 255 (1) (2011) 48–56.
[59] J. Sun, M. Shannon, Y. Ando, L.K. Schnackenberg, N.A. Khan, D. Portilla, R.D. Beger, Serum metabolomic profiles from patients with acute kidney injury: a pilot study, J. Chromatogr. B 893–894 (2012) 107–113.
[60] B. Hocher, J. Adamski, Metabolomics for clinical use and research in chronic kidney disease, Nat. Rev. Nephrol. 13 (5) (2017) 269–284.
[61] Y.Y. Zhao, Metabolomics in chronic kidney disease, Clin. Chim. Acta 422 (2013) 59–69.
[62] Z.H. Zhang, J.R. Mao, H. Chen, W. Su, Y. Zhang, L. Zhang, D.Q. Chen, Y.Y. Zhao, N.D. Vaziri, Removal of uremic retention products by hemodialysis is coupled with indiscriminate loss of vital metabolites, Clin. Biochem. 50 (17) (2017) 1078–1086.
[63] Y.Y. Zhao, X.L. Cheng, F. Wei, X.Y. Xiao, W.J. Sun, Y. Zhang, R.C. Lin, Serum metabonomics study of adenine-induced chronic renal failure in rats by ultra performance liquid chromatography coupled with quadrupole time-of-flight mass spectrometry, Biomarkers 17 (1) (2012) 48–55.
[64] Y.Y. Zhao, J. Liu, X.L. Cheng, X. Bai, R.C. Lin, Urinary metabonomics study on biochemical changes in an experimental model of chronic renal failure by adenine based on UPLC Q-TOF/MS, Clin. Chim. Acta 413 (5–6) (2012) 642–649.
[65] Y.Y. Zhao, Y.L. Feng, X. Bai, X.J. Tan, R.C. Lin, Q. Mei, Ultra performance liquid chromatography-based metabonomic study of therapeutic effect of the surface layer of *Poria cocos* on adenine-induced chronic kidney disease provides new insight into anti-fibrosis mechanism, PLoS One 8 (3) (2013) e59617.
[66] A. Fiebeler, J.K. Park, D.N. Muller, C. Lindschau, M. Mengel, S. Merkel, B. Banas, F.C. Luft, H. Haller, Growth arrest specific protein 6/Axl signaling in human inflammatory renal diseases, Am. J. Kidney Dis. 43 (2) (2004) 286–295.
[67] C.V. Rothlin, E.A. Carrera-Silva, L. Bosurgi, S. Ghosh, TAM receptor signaling in immune homeostasis, Annu. Rev. Immunol. 33 (1) (2015) 355–391.
[68] K. Itoh, T. Chiba, S. Takahashi, T. Ishii, K. Igarashi, Y. Katoh, T. Oyake, N. Hayashi, K. Satoh, I. Hatayama, M. Yamamoto, Y. Nabeshima, An Nrf2/small Maf heterodimer mediates the induction of phase II detoxifying enzyme genes through antioxidant response elements, Biochem. Biophys. Res. Commun. 236 (2) (1997) 313–322.
[69] Y.J. Day, L. Huang, H. Ye, J. Linden, M.D. Okusa, Renal ischemia-reperfusion injury and adenosine 2A receptor-mediated tissue protection: role of macrophages, Am. J. Physiol. Renal. Physiol. 288 (4) (2005) F722–F731.
[70] X.M. Meng, D.J. Nikolic-Paterson, H.Y. Lan, Inflammatory processes in renal fibrosis, Nat. Rev. Nephrol. 10 (9) (2014) 493–503.
[71] W. Lv, G.W. Booz, Y. Wang, F. Fan, R.J. Roman, Inflammation and renal fibrosis: recent developments on key signaling molecules as potential therapeutic targets, Eur. J. Pharmacol. 820 (2018) 65–76.
[72] H. Haghi-Aminjan, B. Farhood, M. Rahimifard, T. Didari, M. Baeeri, S. Hassani, R. Hosseini, M. Abdollahi, The protective role of melatonin in chemotherapy-induced nephrotoxicity: a review of non-clinical studies, Expert Opin. Drug Metabol. Toxicol. 14 (9) (2018) 937–950.
[73] R.J. Reiter, D.X. Tan, C. Osuna, E. Gitto, Actions of melatonin in the reduction of oxidative stress. A review, J. Biomed. Sci. 7 (6) (2000) 444–458.
[74] N. Ahmadiasl, S. Banaei, A. Alihemmati, B. Baradaran, E. Azimian, The anti-inflammatory effect of erythropoietin and melatonin on renal ischemia reperfusion injury in male rats, Adv. Pharmaceut. Bull. 4 (1) (2014) 49–54.